Brazilian Journal of Geophysics (2021) 39(2): 197–207

ISSN 0102-261X
www.rbgf.org.br
DOI: 10.22564/rbgf.v38i4.2083

ESTIMATING SEISMOMETER ORIENTATIONS FROM TELESEISMIC P-WAVE PARTICLE MOTION ANALYSIS

Diogo Farrapo Albuquerque[1]*, Marcelo Peres Rocha[1], Marco Ianniruberto[2], George Sand França[1], Reinhardt A. Fuck[2], Matheus Figueredo de Paulo[1], Marcos Breno Aguiar[1], Marcelo Bianchi[3], Marcelo Assumpção[3] and Lucas Vieira Barros[1]

ABSTRACT. Three-component seismometers are essential for seismological methods that demand rotational transformations on the horizontal components. In order to verify the orientation of seismometers installed on Pantanal, Chaco and Paraná Structural Studies Network (XC-USP) and on Seismological Observatory Network (OS-UnB), we used P-wave Particle Motion Analysis combined with Directional Statistics. We also tested this method in a well-known misoriented station (IU.RCBR), which belongs to the Global Seismograph Network (IU-GSN). In addition to station IU.RCBR, with orientation error of +55.80º, we detected 3 stations with errors larger than ±10º: OS.FUN1 (-10.14º), OS.SIM2 (-11.93º) and OS.SSV2 (-27.16º). The orientation error of the last one was possibly caused by the non-declination of the compass used to align the sensor with respect to the geographic north.

Keywords: orientation analysis, seismographic station, three-component seismometer.

RESUMO. Sismômetros triaxiais são essenciais para métodos sismológicos que exigem transformações rotacionais nas componentes horizontais. Para verificar a orientação dos sismômetros instalados na Rede de Estudos Estruturais do Pantanal, Chaco e Paraná (XC-USP) e na Rede do Observatório Sismológico (OS-UnB), foi utilizada a Análise de Movimento de Partículas de ondas P combinada com Estatística Direcional. Também testamos esse método em uma estação com erro de orientação bem conhecido (IU.RCBR), que pertence à Rede Sismográfica Global (IU-GSN). Além da estação IU.RCBR, com erro de orientação de +55.80º, detectamos 3 estações com erros maiores que ±10º: OS.FUN1 (-10,14º), OS.SIM2 (-11,93º) e OS.SSV2 (-27,16º). O erro de orientação da última foi possivelmente ocasionado pela não declinação da bússola utilizada para alinhar o sensor em relação ao norte geográfico.

Palavras-chave: análise de orientação, estação sismográfica, sismômetro triaxial.

Corresponding author: Diogo Farrapo Albuquerque

[1]Universidade de Brasília (UnB), Observatório Sismológico, Campus Universitário Darcy Ribeiro, Prédio SG-13, Phone: +55 (61) 3107-0912, 70910-900, Brasília, DF, Brazil – E-mails: diogofarrapo@gmail.com, marcelorocha@unb.br, georgesand@unb.br, matt.figueredo@gmail.com, marcosaguiar@aluno.unb.br, lucas@unb.br

[2]Universidade de Brasília (UnB), Instituto de Geociências (IG), Campus Universitário Darcy Ribeiro, Phone: +55 (61) 3107-1205, 70910-900, Brasília, DF, Brazil – E-mails: ianniruberto@unb.br, reinhardt@unb.br

[3]Universidade de São Paulo (USP), Instituto de Astronomia, Geofísica e Ciências Atmosféricas (IAG), Centro de Sismologia, Rua do Matão, 1226 - Cidade Universitária, Phone: +55 (11) 3091-4755, 05508-090, São Paulo, SP, Brazil – E-mail: m.bianchi@iag.usp.br, marcelo@iag.usp.br

INTRODUCTION

Three-component seismometers are essential for modern seismological methods, such as earthquake source investigations, receiver functions, S and surface wave tomography, seismic anisotropy and polarization studies. For these methods, it is mandatory to perform rotational transformations of the horizontal motion components, which depends on the correct seismometer alignment to the geographic north (Ekstrom & Busby, 2008).

The most commonly used tool to align seismometers is the magnetic compass, which demands specific declination correction based mainly on the International Geomagnetic Reference Field (IGRF). Excluding the presence of magnetic rocks nearby the station or local site effects, errors can be introduced when declination adjustment is not done, when this adjustment is made in the opposite sense or the declination of another location is applied (Ekstrom & Busby, 2008).

It is also common that reorientations are not performed, during maintenance, because the seismometers, even for temporary networks, are often buried or due to economic issues (e.g. travel costs, accommodation of technicians, fuel). Besides, information about sensor reorientation or replacement is not usually available in metadata files or in field reports. Therefore, it is fundamental to verify the orientation after seismometer deployment or replacement using computational methods.

The consequence of misoriented stations varies for each seismological method and depends on the method sensitivity to incorrect component rotation. Receiver functions (Ammon, 1991; Ligorría & Ammon, 1999), for example, demand a correct horizontal component rotation to isolate the crustal structure bellow the station and calculate Moho depth and the velocity ratio of P and S waves (Vp/Vs). When the seismometer is misoriented, the results of those parameters are unreliable and would lead to uncertain geological interpretations in crustal studies.

With that in mind, the main goal of this study is to verify the orientation of seismometers deployed at 67 stations from two networks: XC-USP (Pantanal, Chaco and Paraná Structural Studies Network of University of São Paulo, 38 stations) and OS-UnB (Seismological Observatory of University of Brasília Network, 29 stations). To test the accuracy of P-wave Particle Motion Analysis, we also used a known misoriented station (RCBR), belonging to IU-GSN (Global Seismograph Network). Figure 1 shows the location of all stations used in this work.

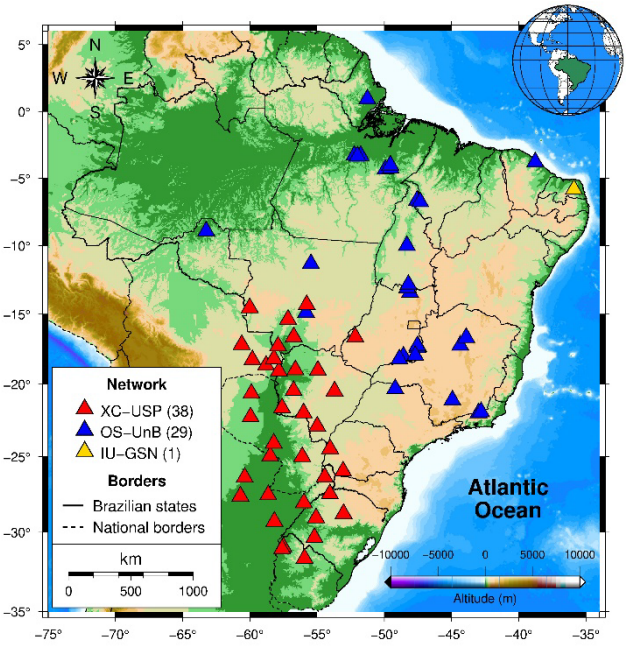

Figure 1 - Location of XC-USP, OS-UnB and IU-GSN stations. The number of stations of each network is indicated in parentheses.

METHODS

The P-wave Particle Motion (PPM) is based on the polarization of seismic waves along the direction of the ray path. This particularity makes possible to decompose the horizontal P arrival vector, recorded in a triaxial station, into vertical, radial and tangential components (Bormann et al., 2012).

The radial and tangential components are obtained by the rotation of the original horizontal components of the seismogram (N: North-South, E: East-West) using the back-azimuth. The Radial component (R) points to the epicenter direction, while the Tangential (T) is orthogonal

to the Radial (Fig. 2). This change in the coordinate system is applied to many seismological methods and relies on the correct orientation of seismometers in relation to the geographic north.

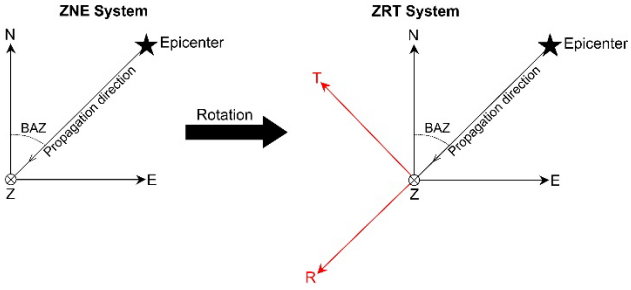

Figure 2 - Rotation to the system ZNE (Vertical, North-South and East-West) to ZRT (Vertical, Radial and Tangential), where BAZ is the back-azimuth.

Using both polarity and amplitude of P-waves in three-component seismograms, it is possible to estimate the back-azimuth (Fig. 2), defined as the angle, in relation to the geographic north, of the surface projection of a seismic ray that connects the source and the receiver along the great circle path (Havskov et al., 2012; Wang et al., 2016).

The amplitude of P-wave gives the maximum displacement of the ground on the vertical (Z) and horizontal components (North-South and East-West), while its polarity (up or down) is a consequence of the source mechanism and the position of the station in relation to the fault.

The arrival amplitude of P-waves in the North-South (A_{NS}) and East-West (A_{EW}) components gives the vector magnitude and their polarities (up or down) give the vector sense (positive: North and East; negative: South and West) (Fig. 3). The back-azimuth of the resultant vector given by PPM (θ_{PPM}) is the arctangent of the ratio of amplitudes (in velocity or displacement) on the horizontal components (Eq. 1).

$$\theta_{PPM} = \arctan\left(\frac{A_{EW}}{A_{NS}}\right) \qquad (1)$$

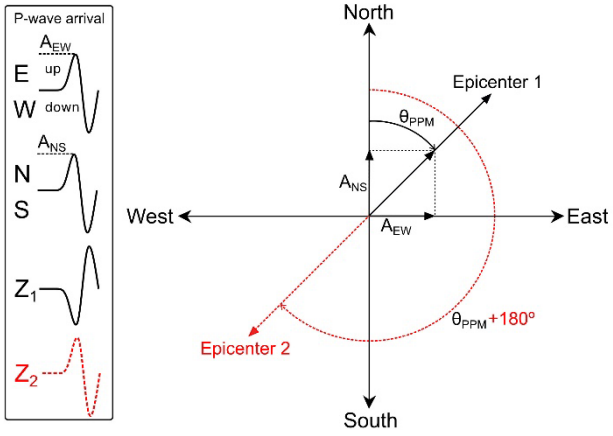

Figure 3 - Determination of back-azimuth using P-wave Particle Motion (θPPM). The inset box indicates the polarity and amplitude of the P-wave arrival in a three-component seismogram (modified from Bormann & Wendt, 2012).

The P-wave polarity on Z solves the ambiguity of 180º of this method. If the arrival on Z is downward, the horizontal particle motion is dilatational and pulls the station towards the Epicenter 1 (Fig. 3). If it is upward, the motion is compressive and pushes the station to the Epicenter 2 (θ_{PPM}+180º) (Havskov et al., 2012).

Using Equation 1 to estimate θ_{PPM} and the theoretical back-azimuth (θ_T), we can calculate the back-azimuth deviation ($\Delta\theta$), defined as:

$$\Delta\theta = \theta_T - \theta_{PPM}. \qquad (2)$$

If $\Delta\theta > 0$, $\Delta\theta$ is clockwise (+). If $\Delta\theta < 0$, $\Delta\theta$ is counterclockwise (-). The theoretical back-azimuth was computed using the coordinates of station and event extracted from the bulletins of Incorporated Research Institutions for Seismology (IRIS).

Figure 3 represents an ideal case, when the P-wave arrival has a very high signal-to-noise ratio (SNR) and it is possible to visually estimate the amplitude, considering the noise close to zero. In real cases, however, it is necessary to use programs that generate PPM diagrams using more than one peak to estimate the back-azimuth.

We used the Particle Motion Tool, implemented on Geotool, to estimate θ_{PPM} by calculating the eigenvectors of the covariance matrix from the horizontal components

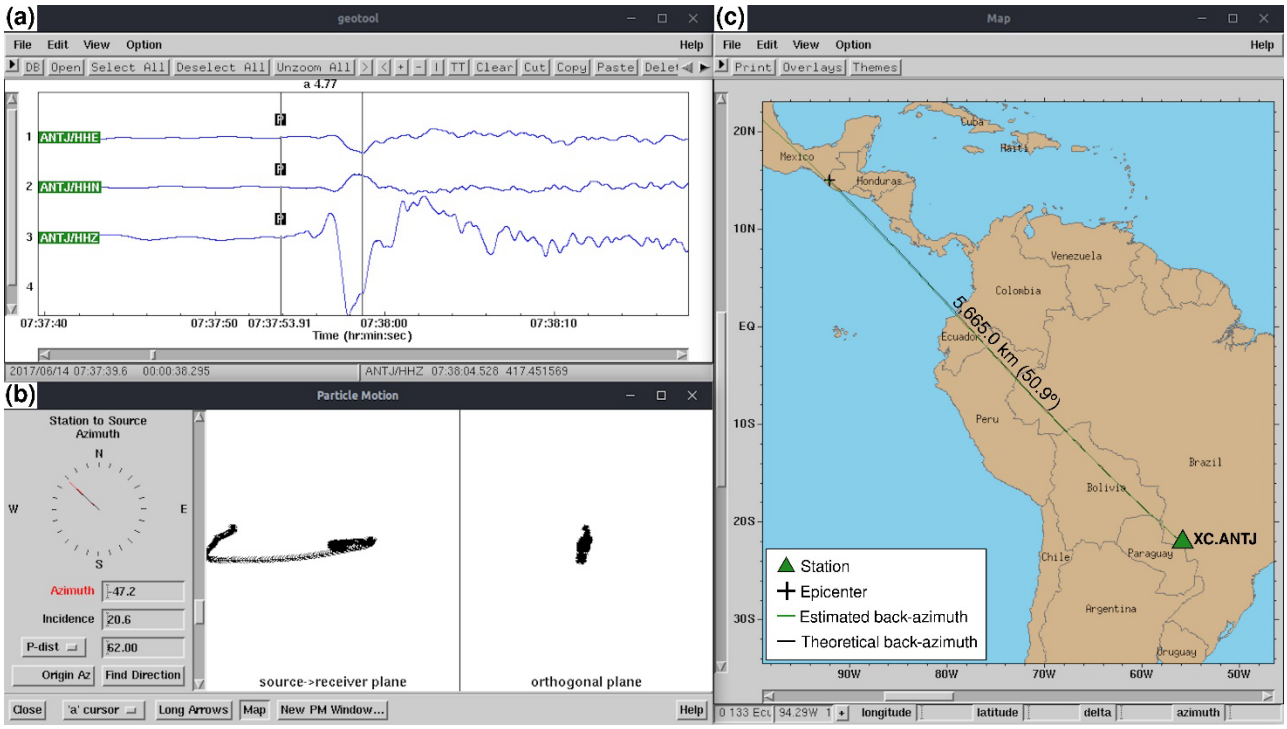

Figure 4 - Geotool windows showing: (a) seismogram recorded by XC.ANTJ station in the three components (HHE: East-West; HHN: North-South; HHZ: Vertical). The first vertical bar indicates the P-wave arrival (07:37:53.91 UTC) and the difference between bars is the time window (4.77 s) used to generate the particle motion; (b) P-wave Particle Motion in the source-to-receiver and orthogonal planes. The estimated back-azimuth (-47.2º) and the P-wave incidence angle (20.6º) are indicated on the left fields; (c) epicenter and station location. The epicentral distance is 5,665.0 km or 50.9º.

(International Data Centre, 2014; Miljanovic 2016; Niu & Li, 2011). Figure 4 shows an example of application of that tool using the three-component seismogram, recorded by XC.ANTJ station, of the earthquake occurred near the border between Mexico and Guatemala on 06/14/2017 at 07:29:05 (Origin Time UTC), with magnitude of 6.9 m_W and depth of 94 km.

The method was applied in the following steps: (1) the P-wave arrival was identified; (2) it was chosen a time window beginning at P-wave arrival and taking, at least, one complete interval between a peak and a trough (Fig. 4a); and (3) the Particle Motion Tool was executed to compute source-to-receiver and orthogonal motions in order to estimate θ_{PPM} and incidence angle (Fig. 4b).

The source-to-receiver represents the vertical plane that contains the source, the receiver (station) and the path of the seismic ray. The orthogonal represents the plane which is orthogonal to the source-to-receiver plane, showing the perspective of a referential looking from the receiver to the source along the ray path (Miljanovic, 2016).

Figure 4c shows the location of the event, the theoretical (-47.0º) and estimated (-47.2º) back-azimuths computed by the Particle Motion Tool. The back-azimuth deviation of -0.2º indicates that XC.ANTJ is not misoriented.

The orientation error (θ_E) was estimated using the circular mean of Directional Statistics. We also tested whether $\Delta\theta$ values were evenly or unimodally distributed using Rayleigh's Test of Uniformity. This test calculates the magnitude of the resultant length vector ($\bar{R}$) and tests it against a random distribution. If $\Delta\theta$ values are tightly clustered, then $\bar{R}$ will be close to 1 and the *p-value* will be less than 0.05. In other words, the test checks whether there is a preferred direction. For most descriptive and inferential purposes, $\bar{R}$ is more important than any measure of dispersion. For more details about Directional Statistics and Rayleigh's Test of Uniformity, see Mardia & Jupp (1999).

The statistical analysis was performed with the Linux version of two R packages: "CircStats" (Agostinelli, 2018) and "circular" (Agostinelli & Lund, 2017).

DATA

The seismological data was provided by the Seismological Observatory at University of Brasília (OS-UnB network), the Seismological Center at University of São Paulo (XC-USP network) and the Incorporated Research Institutions for Seismology (IU-GSN network). The data of OS-UnB and XC-USP networks is not openly available and requires direct permission of these institutions. The data of the RCBR station (IU-GSN) is open and can be downloaded directly from IRIS servers via FDSN, WebRequest or other tools (Albuquerque Seismological Laboratory ASL/USGS, 1988). The metadata information was available in the form of dataless files that can be downloaded directly from the institution websites: www.iris.edu (IU.RCBR) and www.moho.iag.usp.br (XC-USP). The dataless files from OS-UnB stations are not publicly available.

We analyzed 1,095 three-component seismograms, 665 recorded by OS-UnB, from 05/08/2014 to 08/01/2019, and 369 recorded by XC-USP, from 04/16/2016 to 07/12/2019. In terms of unique events, those networks recorded together 189 teleseisms (Fig. 5a).

Three criteria were used in the event selection: (1) epicentral distances ranging from 30º to 100º (Fig. 5b); (2) magnitudes equal or larger than 6.0 (Fig. 5c); and (3) incidence angle of the P-waves, in relation to the normal direction, equal or larger than 10º (Fig. 5e).

As a quality parameter, we used only P-wave arrivals with amplitude of at least twice the RMS amplitude of a 15-second window of background noise in the vertical component and one of the horizontal components. The SNR was computed by the program “sacsnr” available in SACTOOLS package (Thorne, 2017).

Epicenters at distances between 15º and 30º were not selected due to triplications in the upper mantle discontinuities (LeFevre & Helmberger, 1989). Epicentral distances larger than 100º are affected by the P-wave shadow zone (Shearer, 2009). We selected events with magnitude equal or larger than 6.0 because they usually have good SNR and are well located by global networks. The incidence angle criterion was based on a previous analysis of P-wave Particle Motion on the horizontal components, which revealed that arrivals were almost indistinguishable from the background noise when the angle is less than 10º.

The event source parameters (Fig. 5) were extracted from IRIS bulletins. The seismic data was provided by the Seismological Observatory of University of Brasília (SIS-UnB) and Seismology Center of University of São Paulo (USP).

All seismometers installed on XC-USP network are broadband (120 s – 50 Hz and 120 s – 150 Hz) and most of the seismometers installed on OS-UnB network are intermediate (30 s – 100 Hz). The seismometers of OS.COR1, OS.ITU3 and OS.MAN1 are broadband (120 s - 100 Hz) and the seismometers of OS.JQT1, OS.LAJE, OS.SFA1 and OS.SIM2 are short period (1 s – 100 Hz). At IU.RCBR station, there was a broadband borehole seismometer (0.003 Hz – 5 Hz) during the period analyzed.

RESULTS

From the total of 68 stations, we obtained results for 52 (XC-USP: 23; OS-UnB: 28; IU-GSN: 1). The remaining 16 stations recorded less than 5 events with SNR ≥ 2 and it was not possible to reliably estimate θ_E. All results are summarized in Figures 6, 7 and 8.

Figure 6a shows the back-azimuth deviation ($\Delta\theta$) and the mean orientation error (θ_E) estimated for each station of OS-UnB, XC-USP and IU-GSN. Figure 6b shows the $\bar{R}$ variation and the number of events (N) used in the estimates. Figure 7 shows the rose diagrams with $\Delta\theta$ distributions and the indication of θ_E and $\bar{R}$ for each station of OS-UnB (green), XC-USP (blue) and IU-GSN (yellow).

The XC-USP network had no station with θ_E > ±10º (Fig. 6a) or $\bar{R}$ < 0.95 (Fig. 6b). $\bar{R}$ is a measure of angle concentration, which means that XC-USP stations had less dispersion in $\Delta\theta$ or outliers. Rayleigh’s Test of Uniformity indicated

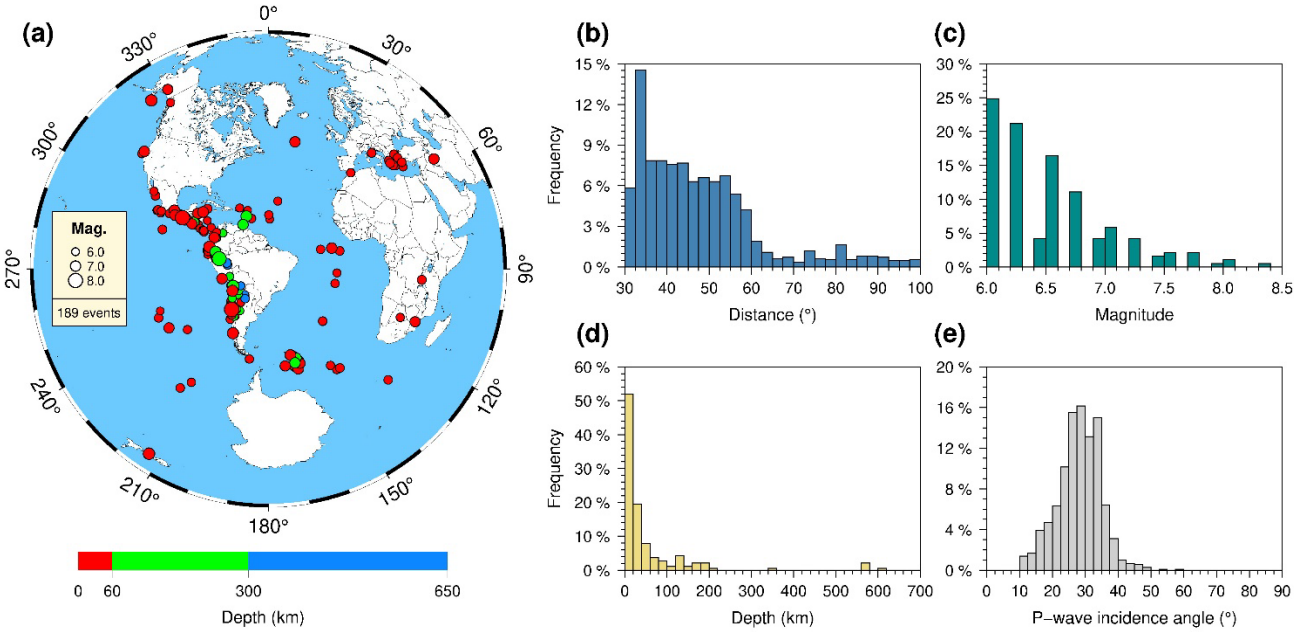

Figure 5 - (a) Location of the events according to their magnitude and depth; (b) Frequency distribution of epicentral distance for all stations; (c) Frequency distribution of magnitudes; (d) Frequency distribution of depth; (e) Frequency distribution of P-wave incidence angle.

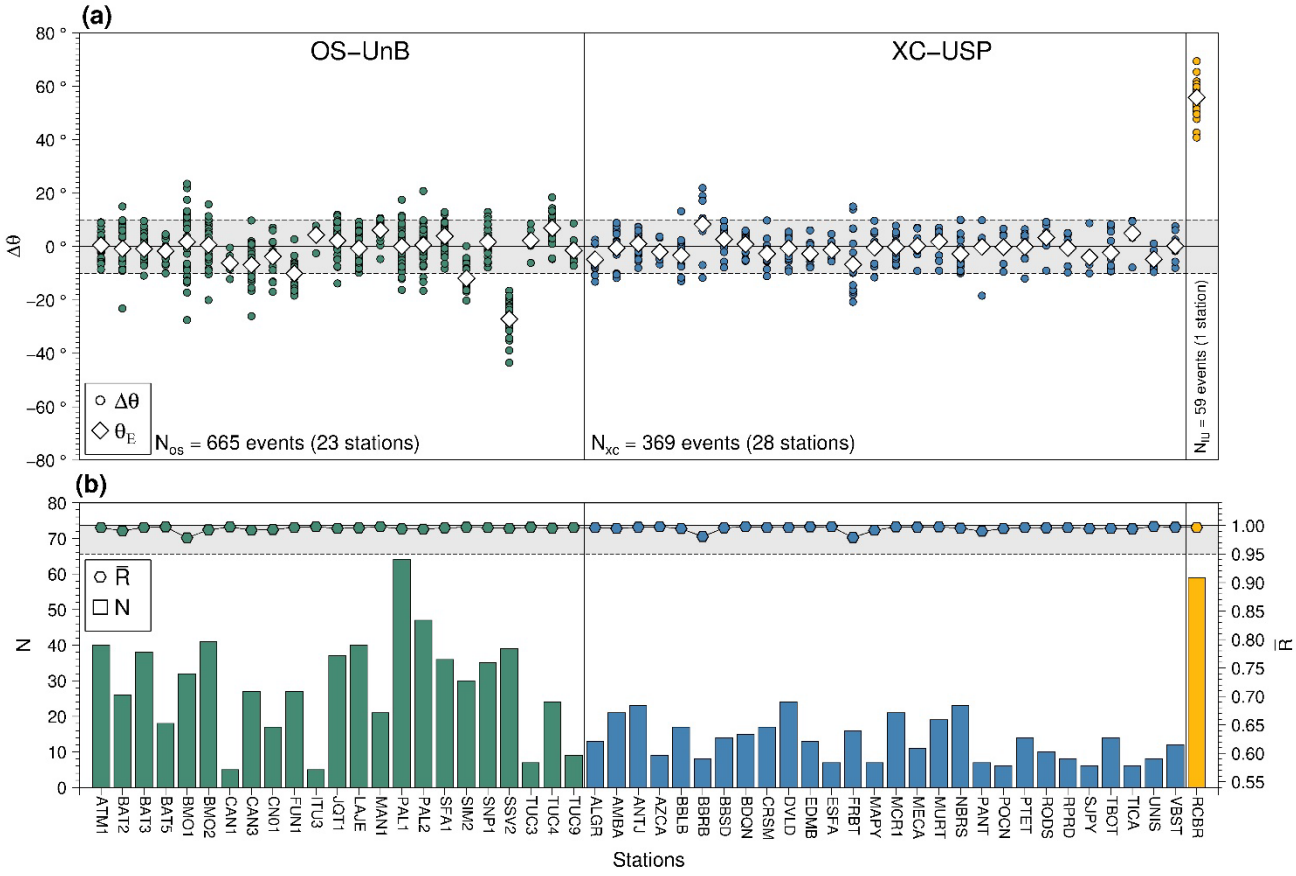

Figure 6 - (a) Back-azimuth deviation (Δθ) and mean orientation error (θ_E) estimated for stations from OS-UnB (green), XC-USP (blue) and IU-GSN (yellow); (b) Resultant length vector ($\bar{R}$) of Δθ for each station; (c) Number of events (N) used to estimate θ_E.

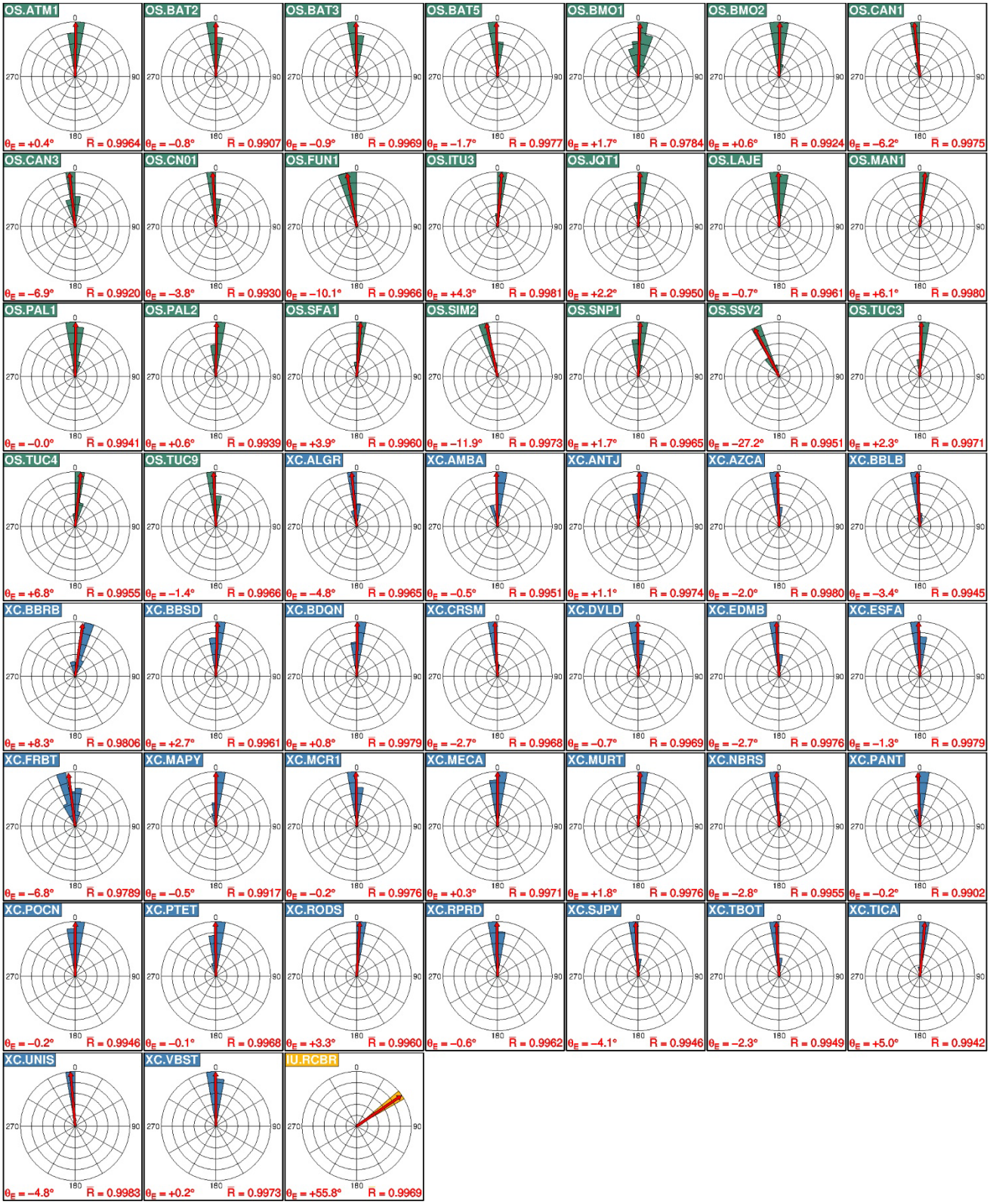

Figure 7 - Rose diagrams for each station from OS-UnB, XC-USP and IU-GSN networks. The colored area, inside the rose, indicates the angular frequency distribution of orientation deviations ($\Delta\theta$) and the arrow indicates the mean orientation error (θE). The value of resultant length vector ($\overline{R}$) is indicated at the right bottom of each diagram.

that $\Delta\theta$ values are unimodally distributed for all the stations of XC-USP ($\bar{R} \approx 1$ and *p-value* < 0.05).

Four stations had θ_E > ±10º: OS.FUN1 (-10.14º), OS.SIM2 (-11.93º), OS.SSV2 (-27.16º) and IU.RSBR (+55.8º) (Figs. 6a, 7 and 8). Rayleigh's Test of Uniformity indicated that $\Delta\theta$ values are unimodal for all the stations of OS-UnB ($\bar{R} \approx 1$ and *p-value* < 0.05). The θ_E informed by the dataless of IU.RCBR is +48º, a discrepancy of 7.8º, probably due to the different methods applied to estimate the orientation.

The standard method to orient borehole seismometers is using a reference triaxial seismometer installed on the surface near the borehole at a known orientation. The horizontal records are then rotated iteratively and correlated with the horizontal borehole records from the same earthquakes. The approximate orientation is obtained when the correlation coefficient reaches the maximum (Trnkoczy et al., 2012).

Although this method seems to be reliable and accurate, there is no detailed analysis describing if it is better than other methods such as PPM. Besides, the difference, between our result and the orientation informed for IU.RCBR, is less than ±10º, which is acceptable for broadband sensors (Bormann et al., 2012).

It is not possible to state that OS.FUN1 and OS.SIM2 are misoriented because the uncertainty, at the moment of seismometer installation, is approximately ±1.5º. This value is based on the propagation of the magnetic compass uncertainty (±0.5º), declination uncertainty of the 12th generation of IGRF (±0.5º) (Thébault et al., 2015) and the uncertainty of the positioning of seismometer, in relation to a reference line, using a protractor (±0.5º). Since magnetic compasses and protractors are analogue devices, the measurement uncertainty is half of the smallest increment (Vuolo, 1996).

For a substantial part of OS-UnB stations, there was no reliable information, in the dataless files or in field reports, about installation date and sensor replacement. Therefore, when that information was not available or not reliable, we had to consider that the same seismometer operated during the whole analyzed period.

In the case of OS.SSV2, for example, we had to consider the first day of available data in the server (11/18/2014) as the deployment date. The IGRF declination for OS.SSV2 coordinates, on that date, was -21.15º, similar to the mean orientation error estimated (-27.16º). This suggests that no declination adjustment was made in the compass to align the OS.SSV2 seismometer, assuming that the difference between the orientation error and the declination (6.01º) was caused mainly by fluctuations in $\Delta\theta$ estimates. It is possible that the technician applied a small clockwise declination, but if we consider that the IGRF declination in the Brazilian territory varies from about -6º to -21º, the hypothesis that no declination was applied makes more sense.

Figure 8 presents the location of all stations and their absolute orientation error ($|\theta_E|$). We used the module of θ_E only for representation purposes.

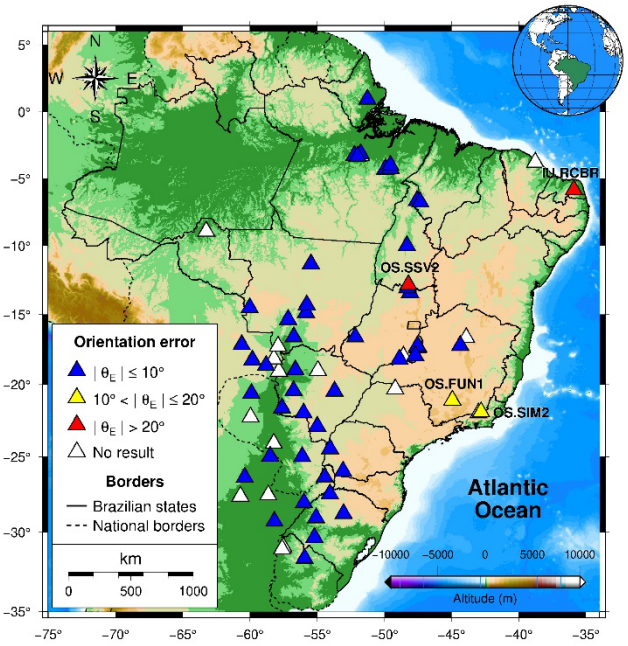

Figure 8 - Location of OS-UnB and XC-USP stations (triangles). The colors indicate the variation of the absolute orientation error ($|\theta_E|$).

When seismograms are broadband, the PPM is linear for a homogenous and isotropic medium, because they tend to be less affected by scattering and diffraction of small-scale heterogeneities in the crust and by topographic slopes nearby the station. The opposite occurs

for short period and intermediate seismograms, making higher frequencies to be more strongly affected by these factors, showing a more elliptical or irregular PPM (Bormann et al., 2012; Buchbinder & Haddon, 1990).

Local site geology may also have an influence on SNR. Seismometers deployed on unconsolidated sediment or soil tend to generate signals with lower SNR compared to seismometers deployed on hard rock outcrops (Trnkoczy et al., 2012). Nonetheless, there was no information about local site geology and we cannot make any assumption about that.

The type of seismometer could be the main cause of the dispersion of $\Delta\theta$ values in most of OS-UnB stations. However, if a short period station has an orientation error of about ±15º, with $\bar{R}$ < 0.95 and *p-value* > 0.05 given by the Rayleigh's Test of Uniformity, we cannot assure that this station is misoriented. Besides, given the properties of arctangent function, small errors in a context of low SNR conditions may result in large back-azimuth deviations, which make the accuracy of θ_{PPM} be highly SNR sensitive (Eisermann et al., 2015).

Therefore, seismometer type and geological conditions influence on SNR and must be took into account to unequivocally indicate which station is misoriented and what may have caused it.

CONCLUSION

The P-wave Particle Motion Analysis, combined with Directional Statistics, proved to be effective to identify possible misoriented stations. We detected 4 stations with mean orientation error larger than ±10º: OS.FUN1 (-10.14º), OS.SIM2 (-11.93º), OS.SSV2 (-27.16º) and IU.RCBR (+55.8º).

All orientation error estimates were computed using at least 5 events with SNR, for P-wave arrivals, twice the noise (for one of the horizontal and vertical components). These criteria, combined with results of the Rayleigh's Test of Uniformity (all stations have $\bar{R}$ > 0.95 and *p-value* < 0.05), assured that the estimates are statistically reliable.

In the case of OS.SSV2, we estimated an orientation error similar to the IGRF declination (-21.15º). Assuming that the difference of 6.01º was caused mainly by fluctuations in $\Delta\theta$ estimates, the result suggests that no declination was applied to the compass.

Since the seismometers of OS-UnB are mostly intermediate and short period, larger dispersions on orientation errors may be caused by diffraction of small-scale heterogeneities in the crust and by topographic slopes nearby the stations.

There was no available information about local site geology and, therefore, it was not possible to verify the effect of unconsolidated sediment or soil on back-azimuth deviations.

REFERENCES

AGOSTINELLI C. 2018. R package "CircStats": Circular Statistics. 45 pp. Available on: <https://cran.r-project.org/web/packages/CircStats/CircStats.pdf>.

AGOSTINELLI C & LUND U. 2017. R package "circular": Circular Statistics. 142 pp. Available on: <https://cran.r-project.org/web/packages/circular/circular.pdf>.

ASL/USGS - Albuquerque Seismological Laboratory. 1988. Global Seismograph Network (GSN - IRIS/USGS). DOI: 10.7914/sn/iu

AMMON CJ. 1991. The isolation of receiver effects from teleseismic P waveforms. Bulletin - Seismological Society of America, 81: 2504–2510.

BORMANN P, ENGDAHL ER & KIND R. 2012. Seismic Wave Propagation and Earth models. In: BORMANN P. (Ed.). 2012. New Manual of Seismological Observatory Practice 2 (NMSOP-2). Potsdam, Germany: Deutsches GeoForschungsZentrum GFZ, 105 pp. DOI: 10.2312/GFZ.NMSOP-2_ch2 Chapter 2. Available on: <https://gfzpublic.gfz-potsdam.de/rest/items/item_65558/component/file_364130/content>.

BORMANN P, KLINGE K & WENDT S. 2012. Data Analysis and Seismogram Interpretation. In: BORMANN P. (Ed.). 2012. New Manual of Seismological Observatory Practice 2 (NMSOP-2). Potsdam, Germany: Deutsches

GeoForschungsZentrum GFZ, 126 pp. DOI: 10.2312/GFZ.NMSOP-2_ch11 Chapter 11. Available on: <https://gfzpublic.gfz-potsdam.de/rest/items/item_257075/component/file_367181/content>.

BORMANN P & WENDT S. 2012. Earthquake location at teleseismic distances from 3-component records. In: BORMANN P (Ed.). 2012. New Manual of Seismological Observatory Practice 2 (NMSOP2). Potsdam, Germany: Deutsches GeoForschungsZentrum GFZ, 18 pp. DOI: 10.2312/GFZ.NMSOP-2_EX_11.2 Exercises 11.2. Available on: <https://gfzpublic.gfz-potsdam.de/rest/items/item_43301_5/component/file_814907/content>.

BUCHBINDER GGR & HADDON RAW. 1990. Azimuthal anomalies of short-period P-wave arrivals from Nahanni aftershocks, Northwest territories, Canada, and effects of surface topography. Bulletin of the Seismological Society of America, 80: 1272–1283.

EISERMANN AS, ZIV A & WUST-BLOCH GH. 2015. Real-Time Back Azimuth for Earthquake Early Warning. Bulletin of the Seismological Society of America, 105: 2274–2285. DOI: 10.1785/0120140298

EKSTROM G & BUSBY RW. 2008. Measurements of Seismometer Orientation at USArray Transportable Array and Backbone Stations. Seismological Research Letters, 79: 554–561. DOI: 10.1785/gssrl.79.4.554

HAVSKOV J, BORMANN P & SCHWEITZER J. 2012. Seismic source location. In: BORMANN P. (Ed.). 2012. New Manual of Seismological Observatory Practice 2 (NMSOP-2). Potsdam, Germany: Deutsches GeoForschungsZentrum GFZ, 36 pp. DOI: 10.2312/GFZ. Information Sheet NMSOP-2_IS_11.1. Available on: <https://gfzpublic.gfz-potsdam.de/pubman/item/item_43361/component/file_816919/IS_11.1_rev1.pdf>.

International Data Centre. 2014. Geotool Design Documentation. Comprehensive Nuclear-Test-Ban Treaty Organization (CTBTO). IDC/SA/SI, 96 pp. Available on: <https://www.ctbto.org/fileadmin/user_upload/procurement/2016/RFQ2016-0139-GEOTOOL_DESIGN_DOCUMENTATION.pdf>.

LEFEVRE LV & HELMBERGER DV. 1989. Upper mantle P velocity structure of the Canadian Shield. Journal of Geophysical Research, 94: 17749. DOI: 10.1029/JB094iB12p17749

LIGORRÍA JP & AMMON CJ. 1999. Iterative deconvolution and receiver-function estimation. Bulletin of the Seismological Society of America, 89: 1395–1400.

MARDIA KV & JUPP PE. 1999. Directional Statistics, Chichester, England: John Wiley & Sons Ltd. 429 pp.

MILJANOVIC V. 2016. Geotool Software User Guide. Comprehensive Nuclear-Test-Ban Treaty Organization (CTBTO). IDC/SA/SI, 217 pp. Available on: <https://www.ctbto.org/fileadmin/user_upload/procurement/2016/RFQ2016-0139-GEOTOOL_SOFTWARE_USER_GUIDE.pdf>.

NIU F & LI J. 2011. Component azimuths of the CEArray stations estimated from P-wave particle motion. Earthquake Science, 24: 3–13. DOI: 10.1007/s11589-011-0764-8

SHEARER PM. 2009. Introduction to Seismology. Cambridge: Cambridge University Press. 442 pp. DOI: 10.1017/CBO9780511841552

THÉBAULT E, FINLAY CC, BEGGAN CD, ALKEN P, AUBERT J, BARROIS O, BERTRAND F, BONDAR T, BONESS A, BROCCO L, CANET E, CHAMBODUT A, CHULLIAT A, COÏSSON P, CIVET F, DU A, FOURNIER A, FRATTER I, GILLET N, HAMILTON B, HAMOUDI M, HULOT G, JAGER T, KORTE M, KUANG W, LALANNE X, LANGLAIS B, LÉGER J-M, LESUR V, LOWES FJ, MACMILLAN S, MANDEA M, MANOJ C, MAUS S, OLSEN N, PETROV V, RIDLEY V, ROTHER M, SABAKA TJ, SATURNINO D, SCHACHTSCHNEIDER R, SIROL O, TANGBORN A, THOMSON A, TØFFNER-CLAUSEN L, VIGNERON P, WARDINSKI I & ZVEREVA T. 2015. International Geomagnetic Reference Field: the 12th generation. Earth, Planets and Space, 67: 79. DOI: 10.1186/s40623-015-0228-9

THORNE M. 2017. SACTOOLS software package. Seismic Analysis Code (SAC). Available

on: <https://github.com/msthorne/SACTOOLS>.

TRNKOCZY A, BORMANN P, HANKA W, HOLCOMB LG, NIGBOR RL, SHINOHARA M, SHIOBARA H & SUYEHIRO K. 2012. Site Selection, Preparation and Installation of Seismic Stations. In: BORMANN P (Ed.). 2012. New Manual of Seismological Observatory Practice 2 (NMSOP-2). Potsdam, Germany: Deutsches GeoForschungsZentrum GFZ, 143 pp. DOI: 10.2312/GFZ.NMSOP-2_ch7 Chapter 7. Available on: <https://gfzpublic.gfz-potsdam.de/rest/items/item_43206/component/file_352734/content>.

VUOLO JH. 1996. Fundamentos da Teoria de Erros. 2nd ed., São Paulo, Brazil: Edgard Blücher. 264 pp.

WANG X, CHEN Q, LI J. & WEI S. 2016. Seismic Sensor Misorientation Measurement Using P-Wave Particle Motion: An Application to the NECsaids Array. Seismological Research Letters, 87: 901–911. DOI: 10.1785/0220160005

D.F.A.: Processing of seismological data, interpretation of results and writing of the manuscript; M.P.R.: Interpretation and review of results and writing of the manuscript; **M.I.:** Interpretation and statistical review of results; **G.S.F.:** Interpretation of results; **R.A.F.:** Interpretation of results and review of the manuscript; **M.F.P.:** Compilation of instrument information; **M.B.A.:** Compilation of instrument information; **M.B.:** Interpretation of results; **M.A.:** Interpretation of results; **L.V.B.:** Interpretation of results.

Received on March 4, 2021 / Accepted on June 2, 2021

Recebido em 4 de março de 2021 / Aceito em 2 de junho de 2021